

Effects of surface wave breaking on the oceanic boundary layer

Hailun He^{1,2} and Dake Chen^{1,3}

Received 10 January 2011; revised 16 February 2011; accepted 22 February 2011; published 15 April 2011.

[1] Existing laboratory studies suggest that surface wave breaking may exert a significant impact on the formation and evolution of oceanic surface boundary layer, which plays an important role in the ocean-atmosphere coupled system. However, present climate models either neglect the effects of wave breaking or treat them implicitly through some crude parameterization. Here we use a one-dimensional ocean model (General Ocean Turbulence Model, GOTM) to investigate the effects of wave breaking on the oceanic boundary layer on diurnal to seasonal time scales. First a set of idealized experiments are carried out to demonstrate the basic physics and the necessity to include wave breaking. Then the model is applied to simulating observations at the northern North Sea and the Ocean Weather Station Papa, which shows that properly accounting for wave breaking effects can improve model performance and help it to successfully capture the observed upper ocean variability. **Citation:** He, H., and D. Chen (2011), Effects of surface wave breaking on the oceanic boundary layer, *Geophys. Res. Lett.*, 38, L07604, doi:10.1029/2011GL046665.

1. Introduction

[2] Oceanic boundary layer (OBL) is the intermediate mixed layer between air and sea, and its dynamics and thermodynamics are essential to the ocean-atmosphere coupled system. Among the physical processes that participate in the air-sea exchange and contribute to the OBL formation and evolution, wind-generated surface waves are considered potentially important but are less studied. How to quantify the effects of surface waves on the OBL is still a challenge.

[3] Laboratory experiments suggest that wave breaking causes significant loss of both momentum and energy fluxes from the wave field [Rapp and Melville, 1990; Melville, 1996; Melville et al., 2002]. The lost momentum flux is transferred to the underlying current, while the lost energy flux is mainly turned to be near-surface turbulence. The breaking-induced turbulence was evident in the dissipation rate near the sea surface which is measured 100 times larger than that from the logarithmic law of the wall [Terray et al., 1996].

[4] In turbulence-resolving models, fine spatial and temporal resolutions are chosen to solve the Navier-Stokes equations, so that the characteristic scales of turbulence are captured directly. This means that such models could be

used to quantify the wave breaking effects. Noh et al. [2004] investigated the effect of the additional stress of wave breaking on the OBL using a three-dimensional Large-Eddy Simulation model, with the stress imposed as a surface boundary condition. Sullivan et al. [2004, 2007] reproduced isolated wave breaking process using direct numerical simulation, and evaluated its effects on the OBL. These turbulence-resolving models all indicate that the wave breaking changes the vertical profiles of the mean current, as well as the turbulent kinetic energy and dissipation. However, the practical use of such models is limited by the required fine resolutions.

[5] In large-scale ocean general circulation models, the sub-grid processes are usually parameterized through a bulk (Reynolds-average) model. Commonly used parameterizations for vertical turbulent mixing do not explicitly account for surface wave field, and the mixing schemes for the OBL are often derived based on the theory of the atmospheric boundary layer [Large et al., 1994]. One exception is Craig and Banner [1994], who considered the energy flux transferred from the wave to the turbulence as a surface boundary condition on the OBL, and establish a theoretical solution. In the same spirits of Sullivan et al. [2004, 2007] and Craig and Banner [1994], here we use a one-dimensional water column model to study the effects of total wave breaking on the OBL on diurnal to seasonal time scales.

2. Model Description

2.1. GOTM

[6] General Ocean Turbulence Model (GOTM) is a one-dimensional water column model [Burchard and Bolding, 2001] (see also <http://www.gotm.net/>), which solves for the transport equations of momentum, heat and salt. The governing equations of GOTM are given by

$$\partial_t u - \partial_z((\nu_t + \nu)\partial_z u) = -g\partial_x \zeta + f v + \tau_{wb,x} \quad (1a)$$

$$\partial_t v - \partial_z((\nu_t + \nu)\partial_z v) = -g\partial_y \zeta - f u + \tau_{wb,y} \quad (1b)$$

$$\partial_t T + u\partial_x T + v\partial_y T + w\partial_z T - \partial_z((\nu'_t + \nu')\partial_z T) = \partial_z I / C_p \rho_0 \quad (1c)$$

$$\partial_t S + u\partial_x S + v\partial_y S + w\partial_z S - \partial_z((\nu'_t + \nu'')\partial_z S) = 0 \quad (1d)$$

where the coordinates are denoted as x (eastward), y (northward), z (upward) and t (time). u , v and w are the eastward, northward and upward velocities respectively. T is the potential temperature, S is the salinity, ν , ν' , ν'' are the molecular diffusivities for momentum, temperature and salinity, respectively; ν_t is the eddy viscosity, ν'_t is the eddy diffusivity; g is the gravitational acceleration, f is the

¹State Key Laboratory of Satellite Ocean Environment Dynamics, Second Institute of Oceanography, Hangzhou, China.

²Key Laboratory of Coastal Disaster and Defense, Ministry of Education, Hohai University, Nanjing, China.

³Lamont-Doherty Earth Observatory, Earth Institute at Columbia University, Palisades, New York, USA.

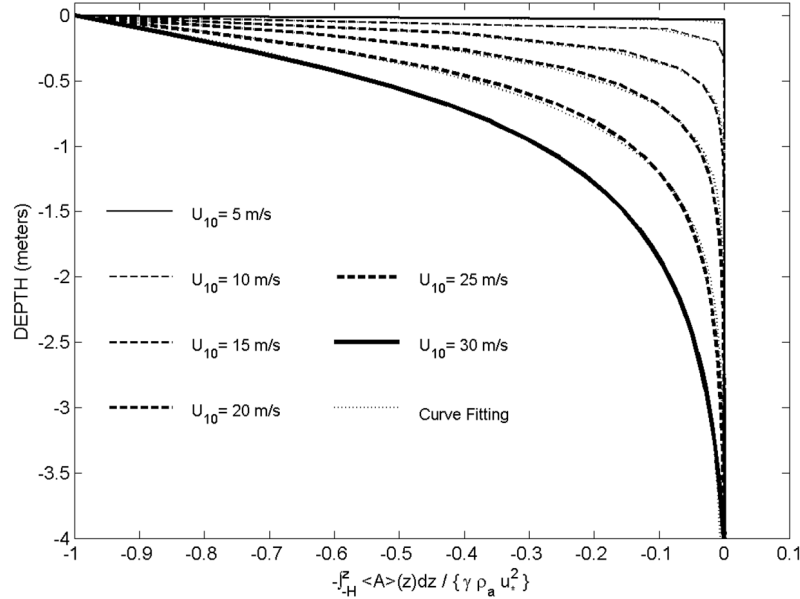


Figure 1. Breaking-induced momentum flux on the water column from bottom $z = -H$ to a given water depth z ($\int_{-H}^z \langle A \rangle(z) dz$), which is normalized by the total breaking-induced momentum flux $\gamma \rho_a u_*^2$. The normalized breaking-induced momentum flux fitted by an exponential function as e^{-bz} , with $b = [100, 22, 6.5, 3.3, 1.9, 1.25]$ corresponding $U_{10} = [5, 10, 15, 20, 25, 30]$ m/s, respectively. U_{10} is the wind speed at the height $z = 10$ m.

Coriolis frequency, I is the solar radiation in the water column, C_p is the specific heat capacity of sea water, ρ_0 is the mean density. In particular, $\tau_{wb} = (\tau_{wb,x}, \tau_{wb,y})$ is the horizontal stress induced by wave breaking, whose direction is aligned with the wind velocity.

[7] For calculating the eddy viscosity and eddy diffusivity, GOTM provides a choice of several second-moment turbulence closure models. We choose *Canuto et al.*'s [2001] “ $k-\varepsilon$ ” two-equation model, which solves for the turbulent kinetic energy (k) and the turbulent dissipation rate (ε) prognostically. *Burchard and Bolding* [2001] compared four second-moment turbulence closure models and showed the advantage of this “ $k-\varepsilon$ ” model on its physical soundness, predictability, computational economy, and numerical robustness.

2.2. Wave Breaking Formula

[8] The wind-driven surface waves can affect the OBL through both wave breaking and Langmuir circulation, with the former mainly caused by the nonlinear wave-wave interaction and the latter by the vortex forces of the Stokes drift. Although the two processes may co-exist and interact [*Sullivan et al.*, 2007], we restrict our attention to the effects of breaking waves in this study. Following *Sullivan et al.* [2004, 2007], the vertical distribution of the wave breaking stress is

$$\tau_{wb}(z) = \langle A \rangle(z) \Delta z \quad (2a)$$

$$\langle A \rangle(z) = \dot{N} \rho_a \iiint P(c) A(x, y, z, t, c) dx dy dt dc \quad (2b)$$

where $\langle A \rangle$ is the momentum density, \dot{N} is the number of breakers created per unit of water surface area per unit of time, ρ_a is the air density, $P(c)$ is the breaking probability

with breaking speed c , and $A(x, y, t, c)$ is the shape function of breaking stress for a single event. $P(c)$ and \dot{N} can be determined by the compatibility conditions [*Sullivan et al.*, 2004, 2007].

[9] The wind stress can be decomposed into two parts: one to the surface waves, and the other to the underlying currents. Surface wave breaking further transfers the wave stress to the currents. So the breaking stress is only a fraction of the wind stress, represented here by

$$\int_{-H}^0 \langle A \rangle(z) dz = \gamma \rho_a u_*^2, \quad (3)$$

where u_* is the atmospheric friction velocity and γ is the ratio of breaking stress out of the wind stress. γ is likely to be dependent on wind speed and wave age [*Papadimitrakis*, 2005], but its functional form is not known and generally the partition mechanism of the wind stress in the ocean is still not clear. Thus we treat γ as a tunable parameter.

[10] It is noted that the computation of equation (2) is time consuming because of the four dimensional integration, so we use the curve fitting method on the vertical decay function as

$$\int_{-H}^z \langle A \rangle(z) dz / \{ \gamma \rho_a u_*^2 \} \approx e^{bz} \quad (4)$$

Figure 1 shows the curve fitting results, which confirms that the curve fitting reduces the time cost without losing the accuracy of vertical distribution. The curve fitting is imposed for wind speeds from 5 to 30 m/s with a 5 m/s interval, and the required vertical distribution function is calculated by linearly interpolation.

[11] The energy flux induced by the wave breaking is formulated as $m_0 \rho_a u_*^3$ with the constant $m_0 = 100$. It is

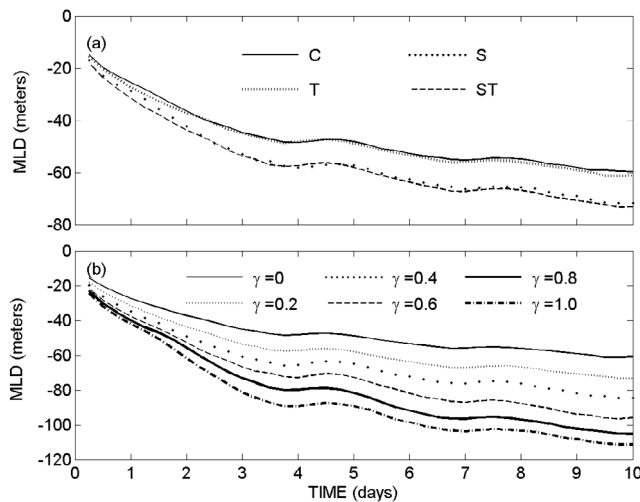


Figure 2. Mixed layer depth (MLD) at 10°N with and without surface wave breaking effects under idealized constant atmospheric forcing (wind stress 0.1 N m^{-2} , surface cooling -50 W m^{-2}). (a) MLD of Case C (control experiment), Case S (breaking-induced stress is considered), Case T (breaking-induced turbulence is considered) and Case ST (both stress and turbulence from breaking are considered). (b) MLD for different γ (the ratio of the breaking-induced stress over the wind stress).

imposed as a surface boundary condition following *Craig and Banner* [1994].

3. Model Experiments

3.1. Mixed Layer Deepening: Steady Atmospheric Forcing

[12] The model response to idealized constant atmospheric forcing is simulated with and without the wave breaking effects. The model location is placed at 10°N , where the inertial period is about 2.9 days. The water depth is set to 200 m. The model is initially at rest with a linear $0.05^\circ\text{C m}^{-1}$ temperature stratification. A constant wind stress of 0.1 N m^{-2} and a constant surface cooling of -50 W m^{-2} are imposed on the air-sea surface. The setup is similar to that used by *Chen et al.* [1994].

[13] The model runs for 10 days, with a vertical resolution of 2 meters. Figure 2a shows the time series of the mixed layer depth (MLD) for cases with and without surface wave breaking, where the MLD is defined as the depth at which the temperature is 0.1°C cooler than the sea surface temperature (SST). Compared with the control experiment (case C, without wave breaking), the experiment with wave breaking (case S, only considering breaking-induced stress) gives much deeper MLD. The different responses of these two cases indicate that the breaking-induced stress largely enhances the vertical turbulent mixing. The similarity between case C and case T (only considering surface turbulent energy input by wave breaking), and that between case S and case ST (considering both the stress and the surface energy input), suggests that the breaking-induced surface energy flux has a relatively small effect on MLD

deepening. SST responses give consistent results, with case S (ST) 0.3°C cooler than case C (T) (not shown).

[14] The parameter γ is set to either 0 (no wave breaking) or 0.2 (wave breaking) for the above experiments. To estimate the model sensitivity to γ , additional experiments are carried out for various values of γ and the results are plotted in Figure 2b. As expected, the larger γ is, the more rapid the initial deepening is, and the deeper the MLD will become.

3.2. Simulation in the Northern North Sea

[15] The data used here were collected as a subset of the PROVESS northern North Sea (NNS) experiment, which lasted from September to November 1998. Only a period of 20 days from October 7–27 is simulated here, as was by *Bolding et al.* [2002] and *Burchard et al.* [2002]. The central location was at 59.3°N and 1°E , with a mean water depth of about 110 m. The scenario is characterized by strong winds, high surface waves and great surface heat loss. In addition to the surface fluxes of momentum and heat, *Bolding et al.*'s [2002] GOTM simulation considers the barotropic forcing mainly consisting of tides, atmospheric pressure gradients and wind set-up. They also parameterize the horizontal and vertical advection of the temperature and salinity based on available measurement. In the present study we use *Bolding et al.*'s [2002] simulation as the control run, with a resolution of 1 meter.

[16] Figure 3 shows the surface forcing and the temperature profiles of the NNS simulations. It is observed that strong winds and accompanying large heat loss began around the seventh day of the simulation period, and then the thermocline was severely eroded and the upper water column was cooled by a few degrees. In the control run, the thermocline erosion and surface cooling are not as strong as in the observation. In contrast, the simulated temperature structure is much closer to the observation when the surface wave breaking effects are included (case ST, with $\gamma = 0.5$). It is also noted that the dissipation rate near the surface in this case is one order of magnitude larger than that in the control run (not shown). This indicates that the surface wave breaking can intensify the vertical mixing and enhance the entrainment of the thermocline water on short time scales.

3.3. Simulation at the Ocean Weather Station Papa

[17] It is well known that the Ocean Weather Station Papa dataset is ideal for testing one-dimensional ocean models because the station is in a region where the horizontal advection of heat and salt is generally small, and the upper-ocean variability is essentially controlled by local atmospheric forcing [*Martin, 1985; Chen et al., 1994; Large et al., 1994; Burchard and Bolding, 2001*]. We choose year 1966 for our simulation. The model is initialized with the temperature and salinity profiles from observations at the beginning of 1966, and the model resolution is 1 meter. Figure 4 (top) shows the daily averaged net surface heat flux and wind stress magnitude at Papa. An annual cycle is obvious in both heat flux and wind stress observations: from early spring to early fall the ocean gains heat from the atmosphere and the winds are relatively weak, while during the rest of the year the ocean loses heat and the winds are strong.

[18] The observed and simulated temperature profiles are shown in Figure 4 (bottom). The observed temperature exhibits a pronounced annual cycle and some high-

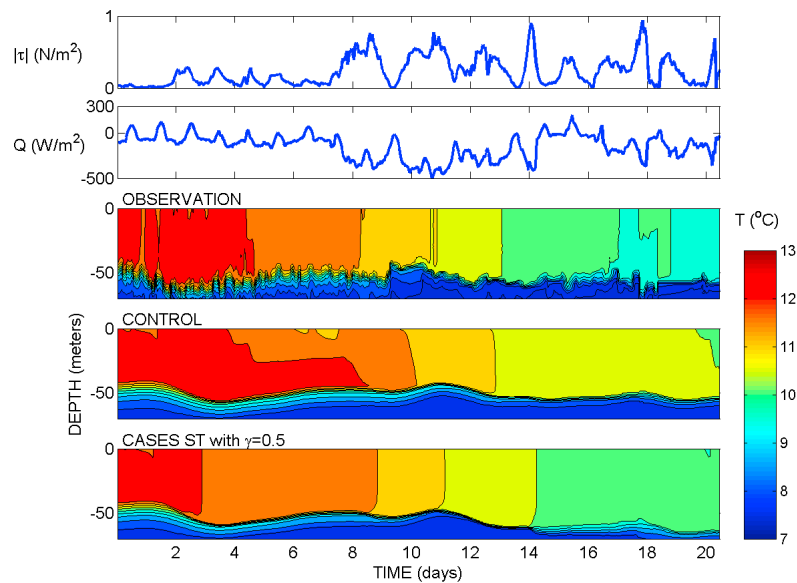


Figure 3. Wind stress magnitude $|\tau|$, net surface heat flux Q , and the simulated temperature profiles in the northern North Sea for a 20-day period starting from 1998-10-07 00:00:00.

frequency fluctuations in response to the atmospheric forcing. Although the observed annual cycle is captured in both numerical tests, the differences between the control and ST (with $\gamma = 0.2$) runs are easily discerned. The control run gives rather shallow MLD during summer months and the SST then is about 3°C too warm as compared to the observations. Moreover, the mixed layer deepening in fall is too slow in the control run, making the SST too warm during this period. In contrast, the seasonal evolution of temperature profile is well simulated in the case with wave breaking effects. The disagreements between model simu-

lation and observation are much reduced when such effects are taken into account.

4. Discussion

[19] It is worth noting that different values of γ are used for the two real simulations described above. As we mentioned earlier, γ should depend on wind speed and wave age. In the absence of an accepted parameterization, it is probably reasonable to use a larger γ for the northern North Sea than for the Ocean Weather Station Papa, since the

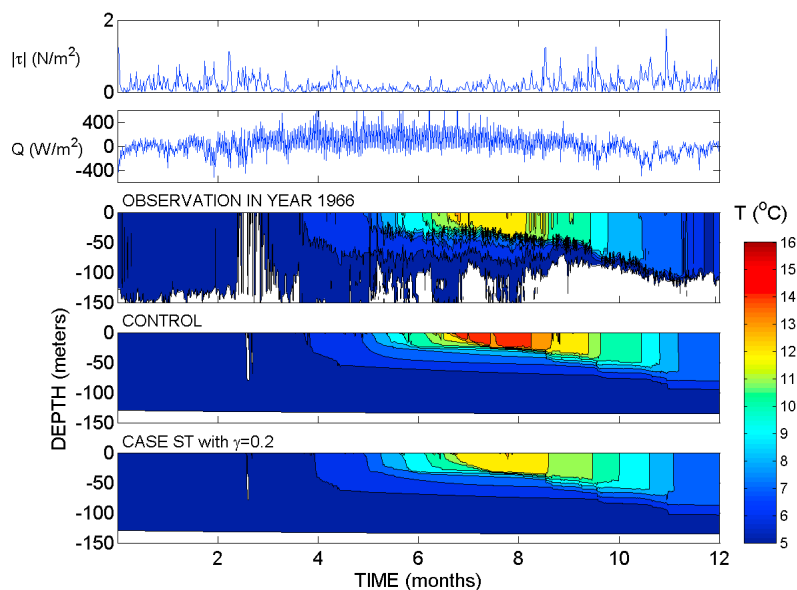


Figure 4. Wind stress magnitude $|\tau|$, net surface heat flux Q , and the simulated temperature profiles at the OWS-Papa for the year of 1966.

mean wind for the short simulation period of the former is much stronger than that for the year-long simulation of the latter. The actual values of γ (0.5 vs. 0.2) are chosen to achieve the best simulations at these two locations that a constant γ would allow. The good agreement between the model results and the observations provides some justification for our choice.

[20] Generally speaking, as a measure of the stress transfer efficiency from surface winds to breaking waves, γ should be a function of space and time, preferably related to some measurable properties of the wind field. For the sake of argument, if at Station Papa we let γ vary with time from 0.2 to 0.5 as a linear function of the wind speed, the simulation shown in Figure 4 would become even more realistic in fall and winter (not shown). A rigorous determination of the functional form of γ will have to come from carefully designed laboratory and field experiments, which surely is an interesting research task but is out of the scope of the present study.

[21] As to the applicability of our wave breaking parameterization, we would argue that even without an accurate estimate of γ , it is still a useful addition to ocean general circulation models. Considering the fact that only part of the surface momentum flux goes to the wave field and that only a portion of the waves would actually break, it may not be unreasonable to assume a constant value of 0.2 for γ in large-scale ocean models. As indicated by our experiments, this value is probably too small for strong winds and rough sea states, but even such a conservative representation of the wave breaking effects can significantly improve model simulations of the OBL.

5. Conclusions

[22] Using the one-dimensional General Ocean Turbulence Model, we have studied the effects of wave breaking on the oceanic boundary layer on diurnal to seasonal time scales. Based on the results from both idealized experiments and real case simulations, we draw the following conclusions:

[23] First, surface wave breaking is an important process for the formation and evolution of the OBL. It enhances the vertical turbulent mixing in the upper ocean, resulting in additional MLD deepening and SST cooling. Its effects are particularly pronounced when surface heating is strong and winds are relatively weak, such as summer time. Ocean general circulation models and coupled climate models should take the effects of surface wave breaking into account.

[24] Second, the effects of surface wave breaking can be parameterized as a surface energy flux in the turbulent kinetic energy equation, or a body force (stress flux) in the mean flow momentum equations, or both. Our experiments indicate that the stress flux scheme is far more effective because it brings surface momentum input down to deeper depths. This explains why the models that treat wave breaking as a surface turbulent energy input still cannot simulate the OBL well.

[25] Finally, with our simplified stress flux scheme, it should be quite feasible to include the effects of surface wave breaking in large-scale ocean and climate models, because they are directly incorporated into the mean flow equations. Even if higher order turbulence closure is not used (i.e., no prognostic turbulent energy calculation), the

main impact of surface wave breaking is well accounted for. We are now in the process of applying the scheme to a general circulation model, and the outcome will be reported on another occasion.

[26] **Acknowledgments.** This work is supported by research grants from the National Basic Research Program (2007CB816005), the National Science Foundation of China (40730843), the National Oceanic and Atmospheric Administration, and the National Aeronautics and Space Administration. Comments and suggestions provided by two anonymous reviewers are greatly appreciated.

[27] The Editor thanks two anonymous reviewers for their assistance in evaluating this paper.

References

- Bolding, K., H. Burchard, T. Pohlmann, and A. Stips (2002), Turbulent mixing in the northern North Sea: A numerical model study, *Cont. Shelf Res.*, *22*, 2707–2724, doi:10.1016/S0278-4343(02)00122-X.
- Burchard, H., and K. Bolding (2001), Comparative analysis of four second-moment turbulence closure models for the oceanic mixed layer, *J. Phys. Oceanogr.*, *31*, 1943–1968, doi:10.1175/1520-0485(2001)031<1943:CAOFMS>2.0.CO;2.
- Burchard, H., K. Bolding, T. P. Rippeth, A. Stips, J. H. Simpson, and J. Sündermann (2002), Microstructure of turbulence in the northern North Sea: A comparative study of observations and model simulations, *J. Sea Res.*, *47*, 223–238, doi:10.1016/S1385-1101(02)00126-0.
- Canuto, V. M., A. Howard, Y. Cheng, and M. S. Dubovikov (2001), Ocean turbulence. Part I: One-point closure model momentum and heat vertical diffusivities, *J. Phys. Oceanogr.*, *31*, 1413–1426.
- Chen, D., L. M. Rothstein, and A. J. Busalacchi (1994), A hybrid vertical mixing scheme and its application to tropical ocean models, *J. Phys. Oceanogr.*, *24*, 2156–2179, doi:10.1175/1520-0485(1994)024<2156:AHVMSA>2.0.CO;2.
- Craig, P. D., and M. L. Banner (1994), Modeling wave-enhanced turbulence in the ocean surface layer, *J. Phys. Oceanogr.*, *24*, 2546–2559, doi:10.1175/1520-0485(1994)024<2546:MWETIT>2.0.CO;2.
- Large, W. G., J. C. McWilliams, and S. C. Doney (1994), Oceanic vertical mixing: A review and a model with a nonlocal boundary layer parameterization, *Rev. Geophys.*, *32*, 363–403, doi:10.1029/94RG01872.
- Martin, P. (1985), Simulation of the mixed layer at OWS November and Papa with several models, *J. Geophys. Res.*, *90*, 903–916, doi:10.1029/JC090iC01p00903.
- Melville, W. K. (1996), The role of surface wave breaking in air-sea interaction, *Annu. Rev. Fluid Mech.*, *28*, 279–321, doi:10.1146/annurev.fl.28.010196.001431.
- Melville, W. K., F. Veron, and C. J. White (2002), The velocity field under breaking waves: Coherent structures and turbulence, *J. Fluid Mech.*, *454*, 203–233, doi:10.1017/S0022112001007078.
- Noh, Y., H. S. Min, and S. Raasch (2004), Large eddy simulation of the ocean mixed layer: The effects of wave breaking and Langmuir circulation, *J. Phys. Oceanogr.*, *34*, 720–735, doi:10.1175/1520-0485(2004)034<0720:LESOTO>2.0.CO;2.
- Papadimitrakis, Y. A. (2005), Momentum and energy exchange across an air-water interface. Partitioning (into waves and currents) and parameterization, *Deep Sea Res., Part II*, *52*, 1270–1286, doi:10.1016/j.dsr2.2005.03.006.
- Rapp, R. J., and W. K. Melville (1990), Laboratory measurements of deep water breaking waves, *Philos. Trans. R. Soc. London, Ser. A*, *331*, 735–800, doi:10.1098/rsta.1990.0098.
- Sullivan, P. P., J. C. McWilliams, and W. K. Melville (2004), The oceanic boundary layer driven by wave breaking with stochastic variability. I: Direct numerical simulation, *J. Fluid Mech.*, *507*, 143–174, doi:10.1017/S0022112004008882.
- Sullivan, P. P., J. C. McWilliams, and W. K. Melville (2007), Surface gravity wave effects in the oceanic boundary layer: Large-eddy simulation with vortex force and stochastic breakers, *J. Fluid Mech.*, *593*, 405–452, doi:10.1017/S002211200700897X.
- Terray, E. A., M. A. Donelan, Y. C. Agrawal, W. M. Drennan, K. K. Kahma, A. J. Williams III, P. A. Hwang, and S. A. Kitaigorodskii (1996), Estimates of kinetic energy dissipation under breaking waves, *J. Phys. Oceanogr.*, *26*, 792–807, doi:10.1175/1520-0485(1996)026<0792:EOKEDU>2.0.CO;2.

D. Chen and H. He, State Key Laboratory of Satellite Ocean Environment Dynamics, Second Institute of Oceanography, No. 36 Baohubei Rd., Hangzhou 310012, China. (hehailun@sio.org.cn)